BIOORGANIC CHEMISTRY 20, 323–333 (1992)

The Molecular Conformation of Chorismic Acid in the Crystalline State

CAROL AFSHAR,* EILEEN K. JAFFE,* H. L. CARRELL,* GEORGE D. MARKHAM,* JAYANTHI S. RAJAGOPALAN,* MIRIAM ROSSI,*,† AND JENNY P. GLUSKER*,[1]

*The Institute for Cancer Research, Fox Chase Cancer Center, 7701 Burholme Avenue, Philadelphia, Pennsylvania 19111; and †Vassar College, Poughkeepsie, New York

Received July 1, 1992

Chorismic acid is the branch point intermediate in the biosynthesis of all aromatic amino acids, and is essential in the metabolism of plants, fungi, and bacteria, but not mammals, making it an attractive target for herbicide, fungicide, or bacteriocide design. Chorismate has attracted substantial attention from bioorganic chemists because it spontaneously rearranges to prephenate in a reaction that is catalyzed 10^6-fold by specific enzymes (chorismate mutases) and up to 10^4-fold by certain catalytic antibodies. The detailed molecular structure of chorismic acid, previously unknown, has been determined by X-ray crystallography. The free acid, formula $C_{10}H_{10}O_6$, crystallizes with orthorhombic space group symmetry $C222_1$ with unit cell dimensions a = 4.569 (1), b = 20.437 (7), c = 29.229 (9) Å, and V = 2729 (1) Å^3. The solvent of crystallization approximates 1.5 H_2O and 0.5 CCl_4 per molecule of chorismic acid. Crystals were unstable at room temperature and therefore X-ray diffraction data were measured at low temperature (−125°C). The phase problem was solved by direct methods and the model was refined by a full-matrix least-squares technique to give a final R = 0.092 and R_w = 0.10. The structure shows the anticipated positions of single and double bonds with typical bond lengths. The conformation of chorismic acid in this crystal structure is *trans* diequatorial with respect to extracyclic groups C(3) and C(4); this is also reported to be the predominant conformer in solution. In this conformation the carbon atoms which become bonded in the enzymatic rearrangement to prephenate are quite distant from one another. This may explain why it was possible to obtain crystals which, although unstable at room temperature, could be studied at lower temperatures.

INTRODUCTION

Chorismic acid is the branch point intermediate in the biosynthesis of the three aromatic amino acids, phenylalanine, tyrosine, and tryptophan (see Fig. 1) (*1, 2*). In bacteria, chorismic acid is also the precursor to the 4-hydroxybenzoate, 4-aminobenzoate, the isoprenoid quinones, vitamin K_1, coenzyme Q, and the folate cofactors. In plants and fungi, chorismic acid is, in addition, a precursor to coumarins, flavonoids, betalains, lignins, and a variety of alkaloids and quinones (*3*). A major biochemical destiny of chorismate is its rearrangement to prephenate via a 3,3-sigmatropic rearrangement as shown in Fig. 2a (*4*). This is the only

[1] To whom correspondence should be addressed.

0045-2068/92 $5.00

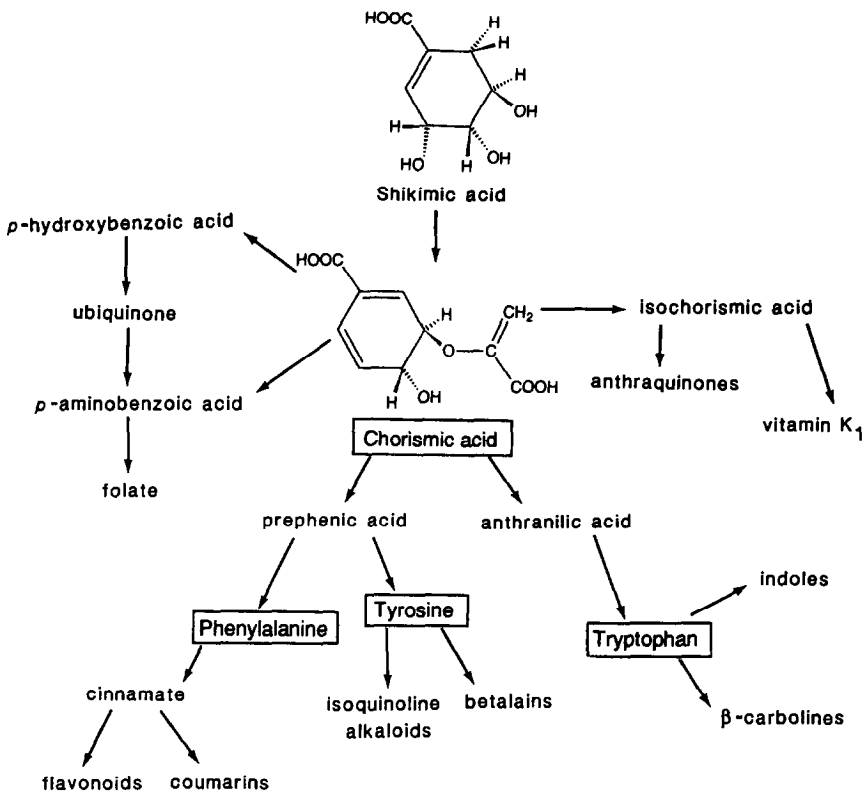

FIG. 1. Scheme of the metabolism of chorismic acid in higher plants.

pericyclic rearrangement known to occur in biological systems. It occurs spontaneously at an unexpectedly high rate, and this reaction has attracted much experimental and theoretical attention (*5, 6*). Immunoglobulins which catalyze the rearrangement of chorismate to prephenate were among the first catalytic antibodies developed (*7*). Because chorismic acid is an essential participant in the metabolism of plants, fungi, and bacteria, but not in mammalian metabolism, an understanding of the structure of chorismic acid can aid in the rational design of herbicides, fungicides, and/or antibiotics (*8*). With this long term goal in mind, we undertook the determination of the crystal structure of chorismic acid.

EXPERIMENTAL

Materials

Chorismic acid was purified from the spent growth medium of *Klebsiella pneumoniae* 62-1 according to the procedure described by Gibson (*9*). Because of the instability of chorismate at various stages of preparation the entire procedure was

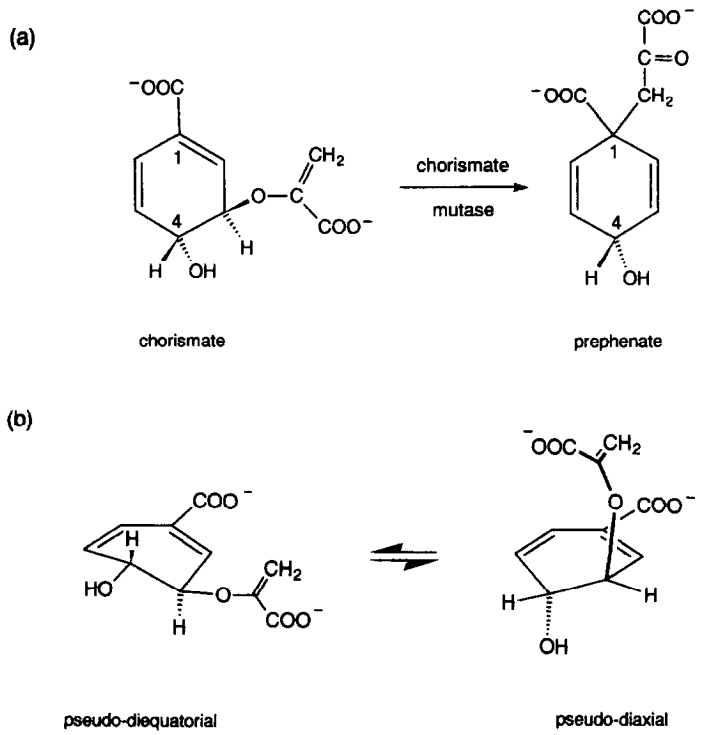

FIG. 2. (a) The rearrangement of chorismate to prephenate, catalyzed by the enzyme chorismate mutase. (b) The pseudo-diequatorial and pseudo-diaxial conformations of chorismate.

carried out in a single day yielding minute crystals of chorismic acid from a diethyl ether/petroleum ether mixture at −20°C. The ^{13}C NMR spectrum of the product was consistent with subsequently published data (*10*). Since the initial preparation, we have both improved the yield of chorismic acid from *K. pneumoniae* 62-1 and simplified the purification protocol, although crystallization of chorismic acid prepared in this manner has not yet been attempted (*10*).

Methods

X-ray data. Crystals were obtained by recrystallization of the minute crystals (described above) from a 50/50 mixture of ethyl acetate and carbon tetrachloride at 4°C; they were not stable at room temperature and tended to melt. Therefore, diffraction data were measured at low temperatures. A colorless crystal with dimensions 0.30 × 0.10 × 0.50 mm was mounted with silicone grease at the end of a glass fiber and placed in a stream of liquid nitrogen for data collection. The low temperature caused the crystal to be bonded rigidly to the fiber. Crystallographic data are listed in Table 1. The X-ray diffraction data were collected on a Nicolet/Siemens P3F update of a $P2_1$ 4-circle automated diffractometer using variable ω scans in the range 2.02–58.6° min^{-1}, depending on reflection intensity.

TABLE 1

Crystallographic Data

Compound	$C_{10}H_{10}O_6 \cdot 1.5H_2O \cdot 0.5CCl_4$
F.W.	330.12
Space group	$C222_1$
a (Å)	4.569 (1)
b (Å)	20.437(7)
c (Å)	29.229(9)
V (Å^3)	2727(1)
Z	8
d_{calc} (Mgm^{-3})	1.607
Temp. (°C)	−125
Radiation	MoKα
μ (cm^{-1})	5.039
Number of independent reflections	1820
Number with $I > 2.5\ \sigma(I)$	905
Final R	0.092
Final R_w	0.10
Number with $I > 3.0\ \sigma(I)$	811
Final R	0.084
Final R_w	0.096

Graphite-monochromatized MoKα radiation (wavelength 0.71069 Å) was used. Cell constants and an orientation matrix for data collection were obtained from a least-squares refinement of 25 well-centered reflections. The data were collected at a temperature of −125°C. The index range for Bragg reflections was $h = 0$ to 5, $k = 0$ to 26, $l = 0$ to 37 to a maximum sin θ/λ of 0.65 Å^{-1}. The total number of independent data is 1820. Four standard reflections were measured at periodic intervals in order to check for crystal decay and no such decay was observed during this low temperature data collection. The data were corrected for Lorentz and polarization effects but an absorption correction was deemed unnecessary ($\mu r = 0.08$). The weights for reflections used in the least-squares refinements, $w = 1/\sigma^2(F)$ were derived from counting statistics using the relation $\sigma(F) = (F/2)[\sigma^2(I)/(I)^2 + \delta^2]^{1/2}$ in which δ (= 0.017 in this study) is an instrumental uncertainty based on variation in the intensities of the standard reflections monitored throughout the data collection. In these two equations w is a number assigned to express the relative precision of each measurement, the integrated intensity (I) is the total intensity measured at the X-ray diffractometer detector when a reflection is scanned, and the structure factor F is the resultant wave scattered by all the atoms of the unit cell relative to the wave scattered in the same direction by a single electron.

Solution and Refinement

The phase problem was solved by direct methods using the program MULTAN80 (*11*). In-house programs were used for all other crystallographic calculations (*12*). Data with intensities I greater than 2.5 $\sigma(I)$ were used in the

analysis. 905 independent reflections were used for the refinement of 183 parameters. All structure refinements on F were carried out using a full-matrix least-squares procedure. The nonhydrogen atoms were refined anisotropically except for the carbon tetrachloride molecule. The atomic scattering factors were taken from International Tables for X-Ray Crystallography (*13*). Hydrogen atom positions were calculated and included, but not varied, in the final refinement using isotropic displacement parameters equal to those of the atoms to which they are bonded. The maximum and minimum electron densities in the final difference Fourier map were 0.56 and -0.45 ($e/\text{Å}^3$), respectively. The R factor is an index that gives a measure of the correctness of a structure and the quality of the data. The final R factors and weighted R factors were $R_{obs} = 0.092$, $R_{all} = 0.198$, $wR_{obs} = 0.100$, $wR_{all} = 0.113$. For data with cutoff of $I > 3\,\sigma(I)$, the values of R_{obs} and wR_{obs} are 0.084 and 0.096, respectively. The final atomic fractional coordinates and averaged displacement parameters are given in Table 2.[2] Atoms H(1) and H(1′) represent alternate positions of the hydrogen atom on a disordered carboxyl group. The numbering of the atoms in this list and for use in the Discussion section is shown for one asymmetric unit in Fig. 3. There are solvent channels through the crystal structure and carbon tetrachloride molecules are disordered in these channels. This disorder affects the precision of the structure determination, since the chlorine atoms of the carbon tetrachloride molecules provide 20% of the scattering power of the unit-cell contents. We were therefore not able to obtain a totally satisfactory model because of the disorder of these molecules in the crystal.

RESULTS AND DISCUSSION

The structure and stereochemistry of chorismic acid obtained from the crystallographic data matches the one proposed by Edwards and Jackman in 1965 (*14*) based on extensive spectroscopic and chemical degradation analyses. The three-dimensional arrangement of atoms is shown as stereopair in Fig. 4. Interatomic distances and angles for this crystal structure are listed in Table 3. The crystal structure analysis unambiguously reveals the geometries of the cyclohexadiene ring and the enol pyruvate side chain; the locations of double bonds in the ring are clear from the interatomic distances (Table 3). The extracyclic substituents on C(3) and C(4) are *trans* to each other and in a pseudo-diequatorial conformation (see Fig. 2b).

The crystal structure also reveals many important aspects of the structure of chorismate that has not been obtained through solution structural studies. The

[2] See NAPS document No. 04988 for 16 pages of supplementary material. Order from ASIS/NAPS. Microfiche Publications, P.O. Box 3513, Grand Central Station, New York, N.Y. 10163. Remit in advance $4.00 for microfiche copy or for photocopy, $7.75 up to 20 pages plus $.30 for each additional page. All orders must be prepaid. Institutions and Organizations may order by purchase order. However, there is a billing and handling charge for this service of $15. Foreign orders add $4.50 for postage and handling, for the first 20 pages, and $1.00 for additional 10 pages of material, $1.50 for postage of any microfiche orders.

TABLE 2

Atomic Coordinates (esd) and Average B (esd)

Atom	x	y	z	B_{av}, B_{iso}(Å)^{2a}
O(1)	1.300 (2)	1.1636 (3)	0.2837 (2)	4.3 (3)
O(2)	1.314 (2)	1.0541 (3)	0.2839 (2)	3.8 (3)
O(3)	0.675 (2)	0.8168 (2)	0.4168 (2)	3.3 (3)
O(4)	0.918 (1)	0.8828 (2)	0.4645 (2)	2.4 (2)
O(5)	0.759 (1)	0.9879 (2)	0.4185 (2)	2.1 (2)
O(6)	0.450 (1)	1.1066 (2)	0.4478 (2)	2.1 (2)
C(1)	1.008 (2)	1.1069 (4)	0.3372 (2)	1.9 (3)
C(2)	0.921 (2)	1.0488 (4)	0.3531 (2)	2.0 (4)
C(3)	0.698 (2)	1.0449 (3)	0.3909 (3)	1.7 (3)
C(4)	0.715 (2)	1.1017 (3)	0.4225 (2)	1.9 (3)
C(5)	0.763 (2)	1.1651 (3)	0.3980 (2)	1.7 (4)
C(6)	0.904 (2)	1.1676 (4)	0.3589 (3)	3.0 (5)
C(7)	0.765 (2)	0.8743 (4)	0.4297 (3)	2.1 (4)
C(8)	0.673 (2)	0.9307 (4)	0.3995 (3)	2.8 (4)
C(9)	0.521 (3)	0.9176 (3)	0.3626 (3)	2.1 (5)
C(10)	1.218 (2)	1.1101 (5)	0.2986 (3)	2.7 (4)
O(W1)	0.225 (2)	1.00000[b]	0.50000[b]	1.9 (3)
O(W2)	0.782 (1)	0.7260 (2)	0.4785 (2)	2.6 (3)
C(T)	0.50000[b]	0.658 (2)	0.75000[b]	10 (1)
Cl(1)	0.099 (3)	0.6765 (5)	0.7537 (6)	7.5 (3)
Cl(2)	0.552 (2)	0.6916 (4)	0.8084 (3)	3.6 (2)
Cl(3)	0.599 (2)	0.5780 (3)	0.7507 (4)	3.2 (2)
Cl(4)	0.609 (3)	0.6990 (5)	0.7110 (3)	5.1 (2)

[a] B_{av} = (1/3) [trace orthogonalized B_{ij} matrix].
[b] Not refined.

C(10) carboxyl group is coplanar with diene portion of the cyclohexadiene ring, as is the C(7) carboxyl group with the C(8)–C(9) double bond; these results are not unexpected in view of the fact that they provide a thermodynamically more favorable arrangement for conjugated double bonds. The enol pyruvic acid side chain on C(3) [C(8)C(9)C(7)O(5)O(3)O(4)] is inclined at an angle of 63.1° to the plane of the carboxyl group on C(1) [(C(10) C(1)O(1)O(2)] and hence of the diene portion of the cyclohexadiene ring.

The one-bond ^{13}C coupling constants ($^1J_{CC}$'s) of chorismic acid have been measured by Rajagopalan and co-workers (*10*) using [U-^{13}C]chorismic acid. Values of $^1J_{CC}$ depend mainly on bond order, bond length, and the attached substituent(s) (*15*). These authors (*10*) noted that the $^1J_{CC}$ value for C(7)–C(8) is 9 Hz larger than that for C(1)–C(10), suggesting that the bond lengths might be different. It was also noted that $^1J_{CC}$ of C(8)–C(9) is 12–14 Hz larger than J_{CC} of C(1)–C(2), J_{CC} of C(5)–C(6), or the comparable $^1J_{CC}$ of a model compound such as acrylic acid. In the crystal structure, the bond length between C(7) and C(8) is almost the same as that between C(1) and C(10). Furthermore, the relative orientation of both the carboxylic acid groups in chorismic acid with respect to the conjugated double

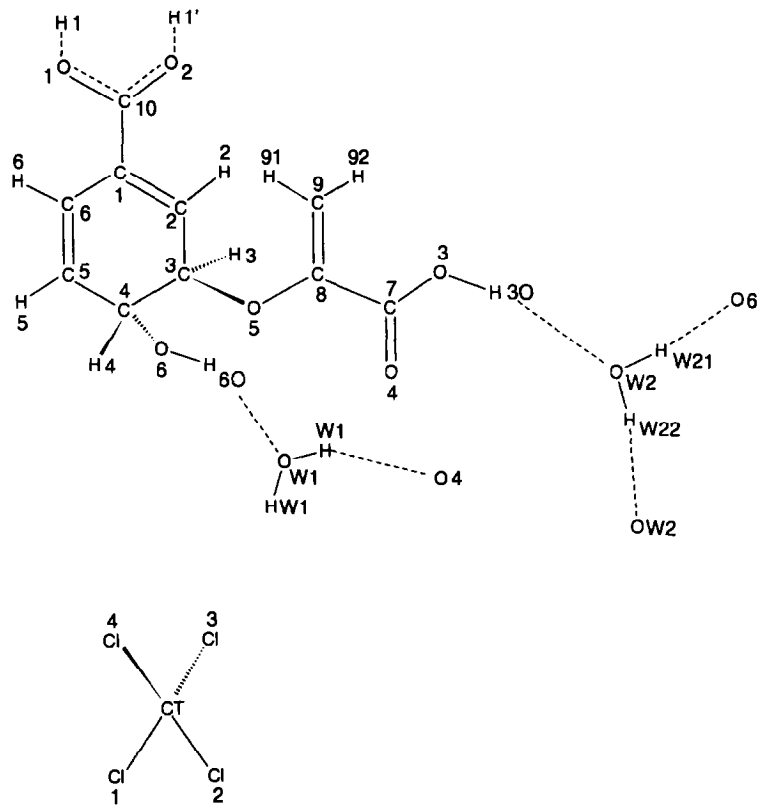

FIG. 3. Atomic numbering scheme of chorismic acid in one asymmetric unit. H(1) and H(1') are only at 50% occupancy due to the disorder of the carboxyl group. The hydrogen-bonding system is also indicated.

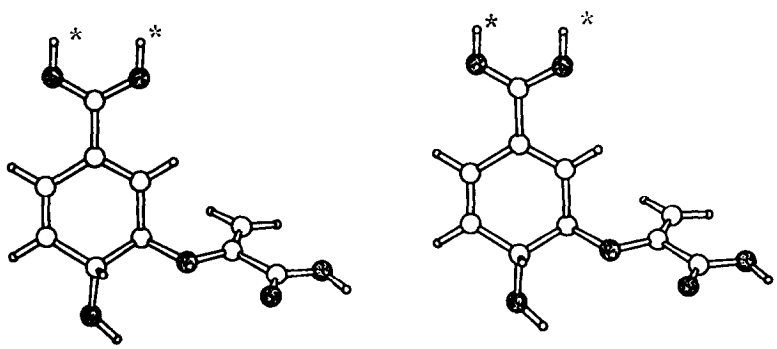

FIG. 4. Stereographic view of the three-dimensional conformation of crystalline chorismic acid in this crystalline form. The asterisks designate disordered hydrogen atoms. Note that H(3) is hidden behind C(3) in this view.

TABLE 3

Bond distances (Å) and Angles (°) with Estimated Standard Deviations in Parentheses

C(1)–C(2)	1.34 (1)	C(8)–C(9)	1.31 (1)
C(1)–C(6)	1.47 (1)	C(8)–C(7)	1.51 (1)
C(1)–C(10)	1.48 (1)	C(7)–O(3)	1.30 (1)
C(2)–C(3)	1.51 (1)	C(7)–O(4)	1.25 (1)
C(3)–C(4)	1.49 (1)	C(10)–O(1)	1.24 (1)
C(3)–O(5)	1.44 (9)	C(10)–O(2)	1.30 (1)
C(4)–C(5)	1.50 (1)	C(T)–Cl(1)	1.87 (1)
C(4)–O(6)	1.42 (9)	C(T)–Cl(2)	1.86 (1)
C(5)–C(6)	1.31 (1)	C(T)–Cl(3)	1.70 (3)
O(5)–C(8)	1.35 (9)	C(T)–Cl(4)	1.50 (2)
C(1)–C(10)–O(2)	115.6 (8)	C(5)–C(4)–O(6)	108.2 (6)
C(1)–C(10)–O(1)	120.2 (8)	C(6)–C(1)–C(10)	120.0 (7)
C(1)–C(2)–C(3)	120.3 (7)	O(5)–C(8)–C(7)	109.8 (7)
C(1)–C(6)–C(5)	120.0 (7)	O(5)–C(8)–C(9)	131.9 (8)
C(2)–C(3)–O(5)	108.8 (6)	C(8)–C(7)–O(4)	121.8 (7)
C(2)–C(3)–C(4)	112.3 (6)	C(8)–C(7)–O(3)	115.6 (7)
C(2)–C(1)–C(6)	120.2 (7)	C(9)–C(8)–C(7)	118.2 (7)
C(2)–C(1)–C(10)	119.8 (7)	O(3)–C(7)–O(4)	122.7 (7)
C(3)–C(4)–O(6)	109.5 (6)	C(1)–C(T)–Cl(2)	89.8 (8)
C(3)–C(4)–C(5)	112.7 (6)	Cl(1)–C(T)–Cl(3)	117 (1)
C(3)–O(5)–C(8)	114.3 (6)	Cl(1)–C(T)–Cl(4)	105 (1)
C(4)–C(5)–C(6)	121.5 (7)	Cl(3)–C(T)–Cl(2)	108.1 (9)
C(4)–C(3)–O(5)	105.8 (6)	Cl(3)–C(T)–Cl(4)	117 (1)
O(1)–C(10)–O(2)	124.1 (8)	Cl(4)–C(T)–Cl(2)	116 (2)

bond is the same. The crystal structure also shows that the bond length between C(8) and C(9) is not dramatically different from the other olefinic bonds. The main difference lies in the effect of substituent on C(8) versus C(1). It is known that electronegative substituents increase one-bond carbon–carbon coupling constants (*15*). Therefore, the differences observed in $^1J_{CC}$ for similar groups in chorismic

TABLE 4

Hydrogen Bonding Scheme

D–H···A	D···A(Å)
O(1)–H(1)···O(1)[a](3 − x, y, ½ − z)	2.687(9)
O(2)–H(1′)···O(2)[a](3 − x, y, ½ − z)	2.611(9)
O(3)–H(30)···OW(2)(x, y, z)	2.633(6)
O(6)–H(60)···OW(1)(x, y, z)	2.851(5)
OW(1)–HW(1)···O(4)(x − 1, y, z)	2.963(6)
OW(2)–HW(21)···O(6)(−x−1, −y, 1½ + z)	2.711(6)
OW(2)–HW(22)···OW(2)(½ + x, ½ − y, 1 − z)	2.786(6)

[a] Representation of a disordered carboxyl group.

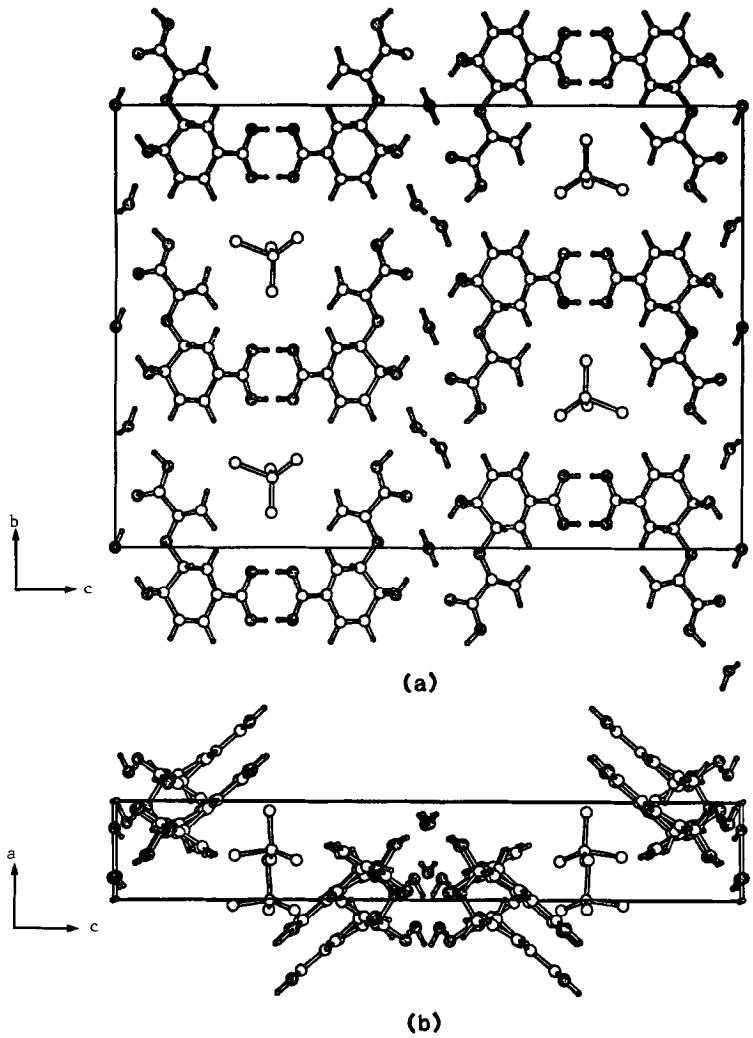

FIG. 5. Crystal packing. (a) View down the *a* axis. (b) View down the *b* axis.

acid provide an example of the effect of the substituents when the bond lengths of the carbon atoms involved are the same.

Copley and Knowles (*16*) have observed from ^{1}H NMR studies that the ratio of the pseudo-diequatorial to pseudo-diaxial conformation is higher in chorismate than in 4-*O*-methyl chorismate; hence they have proposed intramolecular hydrogen bonding between the C(7) carboxylic acid group and the C(4) hydroxyl group as the stabilizing force for the pseudo-diequatorial conformer. In the crystal structure, however, there is no direct hydrogen bonding between the C(7) carboxyl group and the C(4) hydroxyl group; a water molecule OW(2) bridges the two groups between two different chorismic acid molecules (one at x, y, z and the other an a translation away at x-1, y, z) (see Fig. 3).

The packing of molecules in the crystal is illustrated in Fig. 5 which shows the

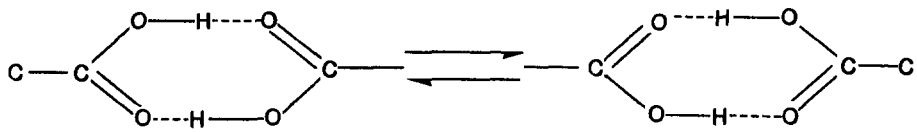

FIG. 6. Hydrogen bonding scheme for the dimer formed by two symmetry-related carboxyl groups [C(10), O(1), O(2)] and disordered hydrogen atoms H(1) and H(1').

carbon tetrachloride and water of crystallization. This figure was drawn by the computer program VIEW (*17*) Fig. 5a is a projection along the short (4.569 Å) axis and Fig. 5b is a projection down the *b* axis of the unit cell. As can be seen in this figure, the carbon tetrachloride lies in a hydrophobic channel, surrounded mainly by C–H groups. These solvent molecules, however, are disordered in this channel and the disorder has hampered the refinement of the structure. Chorismic acid molecules pack together by hydrogen bonding between carboxylic acid groups on C(10), and between the water molecules, carboxyl, carbonyl and hydroxyl groups. This hydrogen bonding scheme is documented in Table 4. The space-group symmetry is such that the carboxyl group C(10), O(1), O(2) is disordered so that it can form a hydrogen-bonded dimer, as shown in Fig. 6. As a result, the hydrogen atoms H(1) [attached to O(1)] and H1′ [attached to O(2)] each have 50% occupancy. The hydrogen bonding scheme of the other carboxyl group shows no evidence of such disorder.

CONCLUSIONS

The conformation of chorismic acid in the crystal studied is the same as that of the predominant conformation in solution: *trans* diequatorial (*16*). The spontaneous rearrangement of chorismate to prephenate in solution has been proposed (*16*) to proceed via the pseudo-diaxial form, not directly from the pseudo-diequatorial form (observed here). This conformational change from pseudo-diequatorial to pseudo-diaxial is important to the action of the enzyme chorismate mutase because it has been proposed to bind the latter in order to facilitate the subsequent rearrangement to prephenate (*16*). Based on ^{1}H NMR studies, the conformational preference of chorismic acid for the pseudo-diequatorial form versus the pseudo-diaxial form is only 4.9 : 1 at 25°C. Chorismic acid is unstable in solution and slowly rearranges to prephenic acid; when heated, chorismic acid also forms *p*-hydroxybenzoic acid, phenylpyruvic acid, and pyruvic acid (*14*). The stability of chorismic acid in the crystalline state at experimental conditions (low temperatures) may be due to the nature of packing of the chorismate molecules in the "less reactive pseudo-diequatorial" conformer in an appropriate environment; there is no apparent contamination by the pseudo-diaxial form, nor were other crystal forms, possibly indicative of a different conformer, observed.

ACKNOWLEDGMENTS

We thank Henry Katz for much assistance during data collection and Drs. David E. Zacharias and John J. Stezowski for their enlightening discussions. This work was supported by National Institutes of Health Grants GM-41913 (E.K.J.), GM-44360 (J.P.G.), CA-10925 (J.P.G.), RR-05539 (I.C.R.), and CA-06927 from the National Institutes of Health and by an appropriation from the Commonwealth of Pennsylvania.

REFERENCES

1. GIBSON, F., AND JACKMAN, L. M. (1963) *Nature* **198,** 388–389.
2. GIBSON, M. I., AND GIBSON, F. (1962) *Biochim. Biophys. Acta* **65,** 160–163.
3. POULSON, C., AND VERPOORTE, R. (1991) *Phytochemistry* **30,** 377–386.
4. GIBSON, M. I., AND GIBSON, F. (1964) *Biochem. J.* **90,** 248–256.
5. ANDREWS, P. R., CAIN, E. N., RIZZARDO, E., AND SMITH, G. D. (1977) *Biochemistry* **16,** 4848–4852.
6. GAJEWSKI, J. J., JURAYJ, J., KIMBROUGH, D. R., GANDE, M. E., GANEM, B., AND CARPENTER, B. K. (1987) *J. Am. Chem. Soc.* **109,** 1170–1186.
7. BOWDISH, K., TANG, Y., HICKS, J. B., AND HILVERT, D. (1991) *J. Biol. Chem.* **266,** 11901–11908.
8. WALSH, C. T., LIU, J., RUSNAK, F., SAKAITANI, M. (1990) *Chem. Rev.* **90,** 1105–1129.
9. GIBSON, F. (1968) *Biochem. Prep.* **12,** 94–97.
10. RAJAGOPALAN, J. S., CHEN, L.-C., AND JAFFE, E. K. (1992) *Bioorg. Chem.* **20,** 115–123.
11. MAIN, P., FISKE, S. J., HULL, S. E., LESSINGER, L., GERMAIN, G., DECLERCQ, J.-P., AND WOOLFSON, M. M. (1980) *MULTAN 80,* A system of Computer Programs for the Automatic Solution of Crystal Structures from X-Ray Diffraction Data, Universities of York, England, and Louvain, Belgium.
12. CARRELL, H. L., SHIEH, H.-S., AND TAKUSAGAWA, F. (1981) The Crystallographic Program Library of The Institute for Cancer Research, Fox Chase Cancer Center, Philadelphia, PA.
13. IBERS, J. A., AND HAMILTON, W. C., (Eds.) (1974) International Tables for X-Ray Crystallography, Vol. IV, Revised and Supplementary Tables to Volumes II and III, The International Union of Crystallography, Kynoch, Birmingham.
14. EDWARDS, J. M., AND JACKMAN, L. M. (1965) *Aust. J. Chem.* **18,** 1227–1239.
15. BREITMAIER, E., AND VOELTER, W. (1987) *in* Topics in Carbon-13 NMR Spectroscopy, VCH, New York.
16. COPLEY, S. D., AND KNOWLES, J. R. (1987) *J. Am. Chem. Soc.* **109,** 5008–5013.
17. CARRELL, H. L. (1976) *VIEW.* Program from The Institute for Cancer Research, Fox Chase Cancer Center, Philadelphia.